

A variable gain physiological controller for a rotary left ventricular assist device

Luis F. V. Silva¹, Thiago D. Cordeiro¹ and Antonio M. N. Lima²

Abstract—This paper deals with designing a physiological adaptive control law for a turbodynamic ventricular assist device (TVAD) using a lumped parameter time-varying model that describes the cardiovascular system. The TVAD is a rotary blood pump driven by an electrical motor. The system simulation also includes the adaptive feedback controller, which provides a physiologically correct cardiac output under different preload and afterload conditions. The cardiac output is estimated at each heartbeat, and the control objective is achieved by dynamically changing the motor speed controller's reference based on the systolic pressure error. TVADs provide support for blood circulation in patients with heart failure. To improve the performance of these devices, several control strategies have been developed over the years, with an emphasis on the physiological strategies that adapt their parameters to improve the patient's condition. In this paper, a new strategy is proposed using a variable gain physiological controller to keep the cardiac output in a reference value under changes in both preload and afterload. Computational models are used to evaluate the performance of this control technique, which has shown better results of adaptability than constant speed controllers and constant gain controllers.

Clinical relevance— This paper shows the importance of computationally simulate adverse conditions of the human cardiovascular system such as changes in preload and afterload in patients under ventricular assist device support. This capability is crucial to quickly evaluate different control strategies in an exhaustive way before in order to choose the most adequate one for a specific patient.

I. INTRODUCTION

Left Ventricular Assist Devices (LVADs) are mechanical devices used to support the blood circulation of patients with heart failure. In order to improve the performance of these devices, several physiological control systems (PCS) approaches have been developed in the early years.

Cordeiro *et al.* [1] developed a physiological control system to adjust the pump ejection pressure at each cardiac cycle maintaining the mean arterial pressure at a specified reference value. A heartbeat detection algorithm based on electrocardiogram signals (ECG) is used to synchronize the control system with the physiological heartbeat. Based on numerical simulation results, one may conclude that the PCS adapted the cardiovascular system (CVS) response to the changes in reference values, defined following the patient's clinical condition.

¹Luis F. V. Silva and Thiago D. Cordeiro are with the Institute of Computing, Federal University of Alagoas, Av. Lourival Melo Mota, 57072-900, Maceió, AL, Brazil {felipemmha, thiago}@ic.ufal.br

²Antonio M. N. Lima is with the Department of Electrical Engineering, Center for Electrical Engineering and Informatics, Universidade Federal de Campina Grande, Rua Aprígio Veloso, 882, 58429-900 Bairro Universitário, Campina Grande, PB, Brazil amnlma@dee.ufcg.edu.br

Another physiological feedback controller for turbodynamic ventricular assist devices (TVADs) based on the recordings of the left ventricular (LV) pressure was developed by Petrou *et al.* [2]. The value of the LV pressure is measured at the inlet cannula of TVAD. The pump inlet pressure (PIP) is used to calculate the LV systolic pressure (SP), which is used to adjust the pump speed of TVAD. The performance of this technique was evaluated on a hybrid mock circulation. Experiments with changing perfusion requirements were compared with the physiological circulation and the pathological one assisted with a constant speed TVAD. However, this control technique has a constant gain and cannot face changes in both preload and afterload.

This paper presents a new physiological controller for a TVAD with a variable gain that adequately react to preload and afterload changes. This variable gain is a function of the error between the actual cardiac output (CO) and a physiological reference (CO_{phy}). All results were obtained using numerical models for both LVAD and CVS models. Moreover, the mechanical dynamics of the TVAD are added, and a PI controller is designed to calculate the pump speed.

II. CVS-LVAD MODEL

The lumped parameter CVS-LVAD model in this work was developed by Simaan *et al.* [3]. It consists of a 6th order nonlinear equivalent circuit that can reproduce the behavior of the left side of the heart, the aortic pressure and flow, the systemic arterial system as well as the blood flow through the LVAD, which is connected between the left ventricle and the aorta (see Fig. 1).

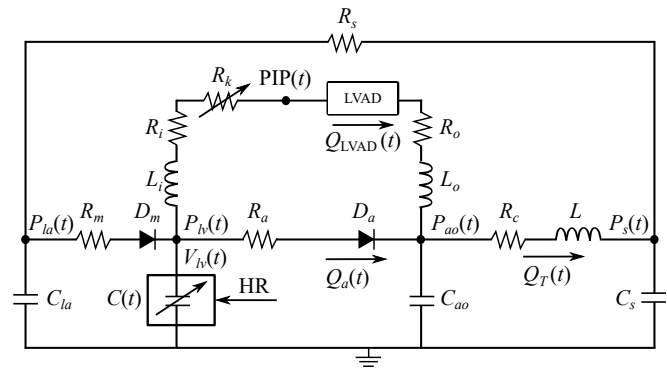


Fig. 1. Equivalent electric circuit representing the CVS-LVAD model

The original formulation of this model uses the left ventricular pressure, $P_{lv}(t)$, as state variable. However, this paper adapted this model to use the left ventricular volume,

$V_{lv}(t)$. This modification was made to not use the derivative of time varying capacitor $C(t)$ avoiding some possible numerical instabilities. Thus, the five state variables of this system without LVAD are: $P_{ao}(t)$, the aortic pressure; $Q_T(t)$, the total flow; $V_{lv}(t)$, the left ventricular volume; $P_s(t)$, the systemic pressure and; $P_{la}(t)$, that is the left atrial pressure. The left atrium is represented by the capacitor C_{la} ; the mitral valve is represented by the resistor R_m and diode D_m ; and the aortic valve is represented by the resistor R_a and diode D_a and the aortic flow is represented by $Q_a(t)$. The behavior of these valves is modeled using ideal diodes taking values of either 1, if valve is open, or 0, if valve is close. The aortic compliance is represented by C_{ao} and the systemic arterial system is modeled using a four-element Windkessel model comprising R_c , L , C_s and R_s . The compliance of the LV is modeled by time-varying capacitor $C(t)$, which is the inverse of elastance function calculated as:

$$E(t) = 1/C(t) = (E_{\max} - E_{\min})E_n(t_n) + E_{\min}, \quad (1)$$

where $E_n(t_n)$ is the normalized elastance called ‘‘double hill’’ function and the parameters E_{\max} and E_{\min} are used to represent the left ventricular condition. The function $E(t)$ is periodic and its period is equal to the cardiac cycle, $t_c = 60/\text{HR}$, where HR is the heart rate [3].

Suga *et al.* [4] described the relationship between left ventricle pressure and volume according to the expression

$$E(t) = \frac{P_{lv}(t)}{V_{lv}(t) - V_o} \quad (2)$$

where V_o is an empirical constant over a wide range of intraventricular volume. By using equation (2), $P_{lv}(t)$ might be calculated as $P_{lv}(t) = E(t)(V_{lv}(t) - V_o)$.

The LVAD used in this work is a rotary blood pump described in [5]. The coupling of this device to the circuit in Figure 1 adds the state, $Q_{LVAD}(t)$, that represents the blood flow through the LVAD. Resistors R_i and R_o and inductors L_i and L_o represents the inlet and outlet resistances and inertances, respectively. The parameter, R_k , is a time-varying, nonlinear, pressure-dependent resistor that simulates the phenomenon of suction and is described as

$$R_k(t) = \begin{cases} \alpha(P_{lv}(t) - P_{lv-suc}), & P_{lv}(t) \leq P_{lv-suc} \\ 0, & \text{otherwise} \end{cases} \quad (3)$$

where α is a LVAD-dependent weight parameter and P_{lv-suc} is a threshold pressure. All parameter values of the CVS-LVAD model and their descriptions are listed in the Appendix. The pressure difference (inlet-outlet) across the pump, H , is defined by the following equation:

$$H = \beta_0 x_6 + \beta_1 \frac{dx_6}{dt} + \beta_2 \omega^2 \quad (4)$$

where ω is the pump speed, and $\beta_0 = -0.17070$, $\beta_1 = -0.02177$ and $\beta_2 = -9.3 \times 10^{-5}$ [5].

The simulations results shown in [3] do not take into account the mechanical dynamics of the pump described in [5]. It is driven by a brushless DC motor described as:

$$J \frac{d\omega}{dt} = T_e - B\omega - T_p \quad (5)$$

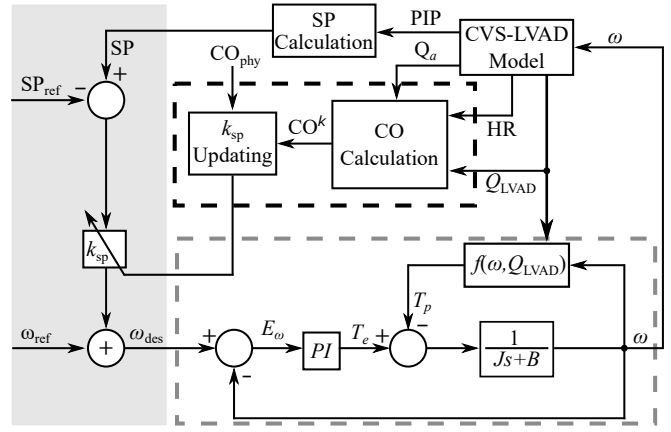


Fig. 2. Block diagram describing the speed update closed-loop (area within the gray dashed line); the k_{sp} updating (area within the black dashed line); and the control law of the SP controller (area with gray background).

where $J = 0.916 \times 10^{-6}$ is the inertia of the rotor, $B = 0.660 \times 10^{-6}$ is the damping coefficient, T_e is the motor torque, and T_p is the load torque on the pump defined as:

$$T_p = f(\omega, Q_{LVAD}) = a_0 \omega^3 + a_1 \omega^2 Q_{LVAD} \quad (6)$$

where $a_0 = 0.738 \times 10^{-12}$ and $a_1 = 0.198 \times 10^{-10}$ are motor model parameters. The block diagram describing the speed update closed-loop can be seen in Figure 2 (see area delimited by a gray line).

III. VARIABLE GAIN SP CONTROLLER

The controller developed by Petrou *et al.* [2] is called SP controller and uses the pump inlet pressure (PIP) to calculate the maximum systolic pressure (SP) which is detected within a fixed time interval of 2 seconds. It is done to ensure that SP value is detected even for low heart rates (Fig. 3). The desired pump speed (ω_{des}) is updated according to:

$$\omega_{des} = k_{SP}(SP - SP_{ref}) + \omega_{ref} \quad (7)$$

where k_{SP} (rpm/mm Hg) is a proportional gain. The values of SP_{ref} (mm Hg) and ω_{ref} (rpm) are reference values obtained during a calibration process described in [2]. This process identifies the pump speed that keeps the desired CO at rest, ω_{ref} , and the corresponding SP, SP_{ref} . The k_{SP} gain can be identified through sensitivity analysis.

The performance of the SP controller was evaluated considering changes in preload, afterload and ventricular contractility. The variables end-diastolic pressure (EDP), CO and SP were observed and compared with reference values previously defined by a physiological response. The results have shown that the behavior of these variables using the SP controller is better than using constant speed. However, the values were not the same as the physiological reference values. Our hypothesis is that this fact occurs because of the constant gain k_{SP} . Moreover, the changes in preload, afterload and ventricular contractility were tested separately, but these changes can co-occur.

To keep the actual value of CO equals to CO_{phy} , in the presence of simultaneous changes of preload and afterload, it

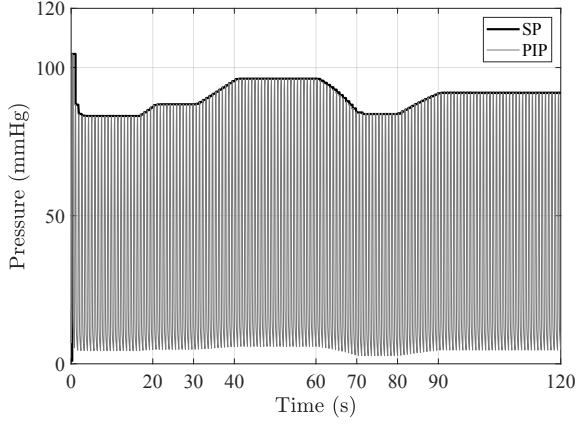


Fig. 3. Systolic pressure (SP) detection using the Pump Inlet Pressure (PIP) signal.

is necessary to make the gain k_{SP} time-varying in (7), which is dependent of the error between CO_{phy} and the current CO .

To accelerate the minimization process of this error signal, E_{CO} , positive and negative thresholds, E_{th}^+ and E_{th}^- were empirically defined. If E_{CO} is greater than E_{th}^+ , it means the k_{SP} value must decrease faster. Thus, its value is updated with a factor that is called of high-threshold Delta (Δ_{high}). However, if E_{CO} is still positive, but smaller than E_{th}^+ , the k_{SP} value is updated with a factor that is called low-threshold Delta (Δ_{low}). For negative values of E_{CO} the idea is similar, but the k_{SP} should be increased. This logic is described in Algorithm 1. The values of the E_{th}^+ and E_{th}^- and the values of Δ_{high} and Δ_{low} are also empirically defined.

In this work, CO is calculated as the integral of the sum of $Q_{LVAD}(t)$ and $Q_a(t)$ and this value is kept constant during one cardiac cycle [7]. Let the k -th cardiac cycle beginning at $t = T_c^k$ and ending at $t = T_c^{k+1}$, for $k = 1, 2, \dots$. The value of CO is only calculated at $t = T_c^k$, CO^k , using the values of $Q_{LVAD}(t)$ and $Q_a(t)$ of the previous cardiac cycle, i.e., from $t = T_c^{k-1}$ to $t = T_c^k$. Hereafter, CO^k is kept constant during the k -th cardiac cycle, i.e, until $t = T_c^{k+1}$. Both discrete and continuous value of CO , CO^k and $CO(t)$, are defined as:

$$CO^k = \left[\int_{T_c^{k-1}}^{T_c^k} (Q_{LVAD}(t) + Q_a(t)) dt \right] \times HR \quad (8)$$

$$CO(t) = CO^k, \text{ for } T_c^k \leq t < T_c^{k+1} \quad (9)$$

In real clinical situations, $CO(t)$ can be obtained by estimation strategies such as the one presented in [7]. It also should be noted that the reference value CO_{phy} is previously defined by experts and can be changed any time.

IV. RESULTS

The preload and afterload variations performed in this paper were done in accord with those described in [3] and can be seen in Figure 4. These changes modify the curves of PIP and SP, as can be seen in Figure 3. These curves are in agreement with those presented in [2]. Another

Algorithm 1: k_{SP} updating

Input: $CO_{phy}^k, CO^k, k_{SP}, \Delta_{high}, \Delta_{low}, E_{th}^+, E_{th}^-$

- 1: $E_{CO} = CO_{phy}^k - CO^k$
- 2: **if** $E_{CO} > E_{th}^+$ **then**
- 3: $k_{SP} = k_{SP} - \Delta_{high}$
- 4: **else if** $0 < E_{CO} < E_{th}^+$ **then**
- 5: $k_{SP} = k_{SP} - \Delta_{low}$
- 6: **else if** $E_{th}^- < E_{CO} < 0$ **then**
- 7: $k_{SP} = k_{SP} + \Delta_{low}$
- 8: **else if** $E_{CO} < E_{th}^-$ **then**
- 9: $k_{SP} = k_{SP} + \Delta_{high}$
- 10: **else if** $E_{CO} = 0$ **then**
- 11: $k_{SP} = k_{SP}$
- 12: **end if**
- 13: **return** k_{SP}

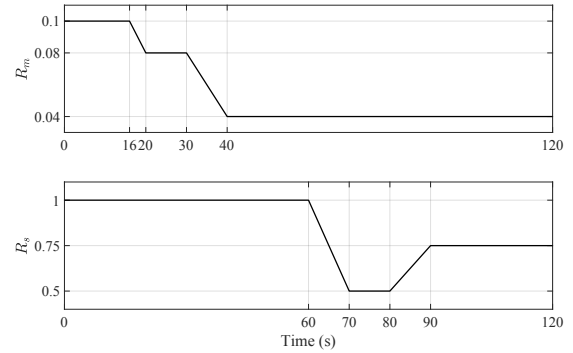


Fig. 4. Preload and Afterload Variation

contribution of this paper is a new real-time strategy to perform SP detection using the first derivative of the filtered PIP signal. This procedure is summarized in Algorithm 2. All numerical simulations were done using the 4th-order Runge–Kutta method in a period of 120 seconds.

Algorithm 2: SP calculation

Input: $PIP^{k-1}, dPIP^{k-1}, P_{ve}^k, L_i, \dot{Q}_{LVAD}^k, R_i, Q_{LVAD}^k$

- 1: $PIP^k = P_{ve}^k - L_i \dot{Q}_{LVAD}^k - R_i Q_{LVAD}^k$
- 2: $dPIP^k = (PIP^k - PIP^{k-1})/h$
- 3: **if** $(dPIP^{k-1} \geq 0 \text{ and } dPIP^k < 0)$ **then**
- 4: $SP^k = PIP^k$
- 5: **else**
- 6: $SP^k = SP^k$
- 7: **end if**
- 8: **return** SP^k

During the calibration process, the pump speed was used to obtain a CO of approximately 3.8 L/min, resulting in $SP_{ref} = 95.19$ mmHg and $\omega_{ref} = 12720$ rpm. With these values, one may define the initial value of the gain $k_{SP} = 20$.

The physiological value of the cardiac output, CO_{phy} , considered for a healthy patient, is the reference target.

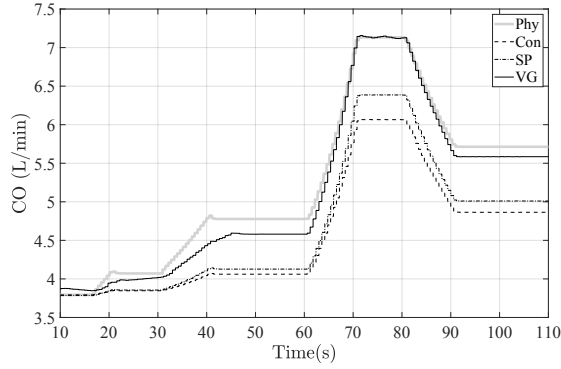


Fig. 5. Comparison between the simulated CO of a healthy patient (CO_{phy}), and a diseased patient with a constant speed controller (CO_{Con}), with the SP controller (CO_{SP}) and with the VG controller (CO_{VG}).

Then, a simulation was performed in order to compare the behavior of CO using the SP controller (CO_{SP}); the constant speed controller (CO_{Con}); and the VG controller (CO_{VG}). The results of these simulations are shown in Figure 5.

The suction phenomenon does not occur by excessive pump speed in all simulations because saturation limits were defined such that k_{SP} has an upper limit of 150 and a lower limit of 1. Although the curve of CO_{SP} is better than the curve of CO_{Con} , there is still a non-zero steady-state error. It also may be seen in Figure 5 that VG controller was able to minimize the error between the CO_{VG} and the desired physiological value CO_{phy} , with minimal steady-state error and in the presence of both preload and afterload changes.

To evaluate the closed-loop stability, one start by fixing the value of the elastance function either at E_{max} or at E_{min} values while keeping constant all the remaining system parameters. Besides, since the speed control loop is stable by design one may consider that $\omega(t) = \omega_{ref}(t), \forall t$. Thus, the closed-loop stability problem is essentially to determine the maximum or the minimum values for k_{sp} such that $\lim_{t \rightarrow \infty} SP(t) = SP_{ref}(t)$, in other words, the lower and upper safety bounds for the output of the k_{sp} updating block. Under these conditions, the CVS-LVAD system is stable for $0 < k_{sp} < 6.5$. The mathematical formulation of this stability test is not shown due to lack of space.

V. CONCLUSIONS

The VG controller presented in this paper is based on that developed in [2], which was tested using a mock circulatory cardiovascular system. The first contribution here is the use of numeric models to reproduce this study, representing changes in preload and afterload, and the expected behavior of control strategies. As a result, a wide range of different strategies and patient conditions can be tested more efficiently. The second contribution is the insertion of the mechanical dynamics of the TVAD that was added along with a PI controller designed to calculate the pump speed.

Although the reference value for the cardiac output, CO_{phy} , has been previously defined, it is not necessarily fixed, i.e., its value can be changed any time for experts. Besides, it

was proved that the proposed control strategy minimizes the steady-state error in the presence of both preload and afterload changes. This fact does not appear using the SP controller, which operates with a constant gain k_{SP} and was tested either for preload or afterload changes.

Another point to be analyzed is the update of the variable gain k_{SP} that can be improved using classical techniques of adaptive control theory or even intelligent techniques. Concerning the values of Δ_{low} and Δ_{high} , other approaches can be evaluated in the future to improve the convergence of the CO, e.g., fuzzy techniques that are capable to change the contribution of these Δ 's. Furthermore, in real situations, the steady-state error can be relaxed for something around $\pm 5\%$. Ultimately, as future work, the detection of the peaks to calculate SP can be improved, eliminating the use of derivatives.

ACKNOWLEDGMENT

The authors would like to thank the financial support provided by PROEX-PPgEE/UFMG and CPG/PROPEP/UFAL.

VI. APPENDIX

$R_s = 1.0$ mmHg/ml: Systemic vascular resistance; $R_c = 0.0398$ mmHg/ml: Characteristic resistance; $R_m = 0.005$ and $R_a = 0.001$ (mmHg/ml): Mitral and Aortic valve resistances; $R_i = 0.0677$ and $R_o = 0.0677$ (mmHg/ml): Inlet and Outlet resistances of cannulae; R_k : Suction resistance with parameters: $\alpha = -3.5$ s/ml and $x_1 = 1$ mmHg; $C_{ae} = 4.4$ ml/mmHg: Left atrial compliance; $C_s = 1.33$ ml/mmHg: Systemic compliance; $C_{ao} = 0.08$ ml/mmHg: Aortic compliance; $L = 0.0005$ mmHg s²/ml: Inertance of blood in aorta; $L_i = 0.0127$ and $L_o = 0.0127$ (mmHg s²/ml): Inlet an outlet inertances of LVAD cannulae.

REFERENCES

- [1] T. D. Cordeiro, D. L. Souza, I. A. Cestari, A. M. N. Lima, A physiological control system for ECG-synchronized pulsatile pediatric ventricular assist devices, *Biomedical Signal Processing and Control*, Mar;57:101752, 2020.
- [2] A. Petrou, G. Ochsner, R. Amacher, P. Pergantis, M. Rebholz, M. Meboldt and M. Schmid Daners, A physiological controller for turbodynamic ventricular assist devices based on left ventricular systolic pressure, *Artificial organs*, Sep;40(9):842-55, 2016.
- [3] M. A. Simaan, A. Ferreira, S. Chen, J. F. Antaki, and D. G. Galati, A dynamical state space representation and performance analysis of a feedback-controlled rotary left ventricular assist device, *IEEE Transactions on Control Systems Technology*, Dec;17(1):15-28, 2008.
- [4] H. Suga and K. Sagawa, Instantaneous pressure-volume relationships and their ratio in the excised, supported canine left ventricle, *Circulation Res.*, vol. 35, no. 1, pp. 117–126, 1974.
- [5] S. Choi, J. R. Boston, D. Thomas and J. F. Antaki, Modeling and identification of an axial flow blood pump. *American Control Conference*, 6:3714-3715, 1997.
- [6] T. Collis, R. B. Devereux, M. J. Roman, G. de Simone, J. L. Yeh, B. V. HowardBV, R.R. Fabsitz, T.K. Welty, Relations of stroke volume and cardiac output to body composition: the strong heart study, *Circulation*, Feb 13;103(6):820-5, 2001.
- [7] A. Petrou, M. Kanakis, K. Magkoutas, B. de Vries, M. Meboldt and M. Schmid Daners, Cardiac Output Estimation: Online Implementation for Left Ventricular Assist Device Support, *IEEE Electron Device Letters*, Dec 2020